

FILE COPY
NO. 1-W

TECHNICAL MEMORANDUMS

NATIONAL ADVISORY COMMITTEE FOR AERONAUTICS

_____ *NACA 672* _____
No. 672

TORSIONAL VIBRATION OF AIRCRAFT ENGINES

By Karl Lürenbaum

Zeitschrift für Flugtechnik und Motorluftschiffahrt
Vol. 23, No. 4, February 29, 1932
Verlag von R. Oldenbourg, München und Berlin

_____ *25* _____
Washington
May, 1932

REPRODUCED BY
NATIONAL TECHNICAL
INFORMATION SERVICE
U. S. DEPARTMENT OF COMMERCE
SPRINGFIELD, VA. 22161

NATIONAL ADVISORY COMMITTEE FOR AERONAUTICS

TECHNICAL MEMORANDUM NO. 672

TORSIONAL VIBRATION OF AIRCRAFT ENGINES*

By Karl Lürenbaum

Exhaustive torsional-vibration investigations are required to determine the reliability of aircraft engines. A general outline of the methods used for such investigations and of the theoretical and mechanical means now available for this purpose is given below, illustrated by examples.

I. VIBRATION CALCULATION

Torsional vibrations in piston engines require particular attention, especially as regards aircraft engines which combine great power and high revolution speeds producing great exciting forces, with low weight and maximum utilization of materials. Frequent crankshaft failures during the last few years have demonstrated in a striking manner the fatal effect of neglected torsional vibrations on safety in operation. Exhaustive vibration investigations are therefore expressly recommended as a means of avoiding undue vibrational stresses by proper precautions.

Calculations, incorporated in the design of power plants, form a large part of the vibration investigation. As a rule, this enables the designer to improve the vibration conditions by appropriate changes. In general, however, a full knowledge of the vibration conditions may be gained only by vibration measurements of the completed engine. Subsequent changes on the basis of vibration measurements are possible only to a limited extent.

The final purpose of practical vibration investigations is the determination of the additional stresses developed by critical vibrations. These investigations are based on the natural vibrations and on the true vibration diagram in any cross section of the vibrating system.

*"Praktische Drehschwingungs-Untersuchung von Luftfahrzeug-Triebwerken." Zeitschrift für Flugtechnik und Motorluftschiffahrt, February 29, 1932, pp. 105-113.

The true vibration diagram shows the amplitude of vibration of a single cross section at the critical points of the operating speed range. The true amplitude of vibration and hence the vibrational stresses can be shown at any point of the vibrating system by the free form of vibration giving the totality of the relative amplitudes of vibration throughout the cross section.

1. Form of Vibration

It was repeatedly shown that, for major critical conditions, free vibrations may be used for stress calculations as a sufficiently accurate equivalent of forced vibrations, provided the system is one of harmonic vibrations with comparatively small natural damping. This condition is fulfilled with sufficient accuracy by standard aviation engines with direct and rigid propeller drive. (Fig. 1.)

Free vibrations and the respective natural vibration members which depend exclusively on the distribution of the masses and springs within the vibrating system, can be calculated by known methods, provided the masses and springs are determinable with sufficient accuracy. The determination of the springs is often difficult. It cannot always be calculated in advance on the basis of design drawings only. As a rule, static torsion tests are required for cranks, bevel couplings, spring couplings, etc. When torsion tests are made with cranks or complete crankshafts, the units should be tested with their bearings and, if possible, with their casings, since the stiffness is greatly affected by the resilience and clearance of the bearings.

Nonharmonic elements of vibrating systems (rubber couplings, Hardy disks, couplings with clearance) somewhat impair the reliability of the vibration calculation, the latter being no longer independent of the amplitude. Yet, according to torsion tests with various nonharmonic couplings, their damping curve does not differ materially from the linear law. In this case the calculation of the form of vibration can be based on a mean damping, namely, that corresponding to the mean torque of the engine.

The determination of the damping effect is much less reliable with geared engines. The gear bearings and casings are incorporated in the elastic system by the transformation of the torque and the resulting reaction of the

driving-gear bearings. This additional damping can be determined only by a torsion test which must be made with the complete engine including the geared parts running in their respective bearings and casings. It cannot yet be determined by calculation. It is hoped that at least an estimate of this influence will be possible in future, as soon as experimental values become available for a larger number of geared engines.

The free form of vibration loses its importance in systems with marked inherent natural damping (vibration damping devices, strongly damping couplings). These systems are not, in general, affected by an increased danger of vibration, since marked resonances can no longer occur. In these cases the stress calculation must no longer be based on the free undamped form of vibration.

2. Vibration Diagram

At present, the course of the true vibration diagram of an engine cannot yet be predicted for the general case. The amplitudes of vibration can be calculated for a known excitation in the noncritical region, the damping forces not having reached their full development (material damping, piston and bearing friction) being thereby neglected. No advantage is gained in this way, since these regions are usually free from any danger of vibration. On the other hand, the amplitudes in the resonance and stress limits cannot be calculated with the required accuracy, no adequate and correct information being yet available as to the magnitude of the damping forces which, in this case, have a decisive influence and balance the exciting forces. Only for the frequently tested 6-cylinder in-line and 12-cylinder V-type engines have damping coefficients been calculated from vibration measurements. Even at the critical points, these coefficients permit expressing the resonance amplitudes of the above engines in satisfactory agreement with their true values. Inasmuch as such coefficients are based on greatly simplified assumptions regarding the true nature of vibration damping, great caution is recommended in using them for similar power-plant arrangements.

While the resonance limits by which the stress calculation is decisively affected must be determined by vibration measurements on the actual engine, at least the relative vibration diagram may be predicted. On the basis of an investigation of the energy devoted by each harmonic of

the total torsional-force diagram to the excitation of vibrations, the series and relative amplitudes of the critical vibrations to be anticipated in the operating speed range can be predicted for any power plant with known number and arrangement of cylinders and cranks, known firing order and form of vibration. This excitation energy is proportional to the resonance amplitude. The curve plotted against the revolution number (r.p.m.) is a relative vibration diagram. Such an investigation was recently made with a large number of four-stroke-cycle aircraft engines by means of a simple graphic method. (Reference 1.)

The relative vibration diagram is a very valuable auxiliary which permits interesting conclusions to be drawn regarding the vibration conditions of a power plant in operation, before its construction has been started, thus affording means for making the necessary changes at the right time. The plotting of the relative vibration curve requires the knowledge of the free form of vibration which cannot always be accurately predicted.

II. VIBRATION MEASUREMENT

Reliable vibration measurements for the determination of the true vibration diagram of aircraft engines were made rather late, because it was necessary to develop adequate measuring instruments and methods. Instruments, hitherto successfully used on low-speed and slowly vibrating stationary and marine power plants, did not yield satisfactory results on aircraft engines.

1. D.V.L. Torsiograph

In the meanwhile the D.V.L. has completed the development of a torsiograph which, in many tests, has been found to meet the particularly difficult conditions of measurement on aircraft engines, giving accurate results up to very high revolution and vibration speeds. The device is designed to be rigidly flanged to a free end of the engine shaft. The vibrations of the free shaft end with respect to a uniformly revolving mass. (principle of the seismograph) are scratched full-scale by a diamond on a moving film. Simultaneously recorded time and revolution marks permit an accurate determination of the position, magnitude, and order of the critical conditions. (Reference 2.) In connection with the concluded develop-

ment and testing of the D.V.L. torsigraph, additional information is given below, illustrated by recent photographs.

The device is built in two sizes (fig. 2):

- a) A large size (diameter of housing 200 mm (7.9 in.));
- b) A small size (diameter of housing 120 " (4.7 ")).

The large type can be used for all large stationary and automobile engines and for aircraft engines down to approximately 200 to 250 hp. In all these cases the vibrating mass of the torsigraph ($\theta = 0.055 \text{ cm kg s}^2$) can be disregarded without error as compared with the vibrating masses of the engines. This is no longer true for small power plants, e.g., aircraft engines of less than 200 hp. The small type was developed for these particular cases. It is, essentially, a geometrical reduction of the large D.V.L. torsigraph. (Fig. 3.) The vibrating mass of the small torsigraph is only about $1/5$ that of the large one and can be safely neglected in comparison with the usual driving-gear masses of small aircraft and automobile engines.

The use of the device was simplified by a distance control consisting of a Bowden wire and a band brake. (Fig. 4.) Measurement at not easily accessible points is thus greatly facilitated. A record with time and revolution marks, magnified 1.5 times, is shown in Figure 5.

2. D.V.L. Torsion Recorder

Vibration measurements at the free end of the shaft are sufficient for the determination of stresses in engines with a clearly defined form of vibration, as, e.g., present-day aircraft engines with direct propeller drive. (Fig. 1.) In the case of geared propellers, driven by the engine through long intermediate shafts, clutches and gears, the form of vibration can no longer be indicated with sufficient accuracy. Its course must be explored with adequate measuring instruments in as many cross sections of the vibrating system as possible.

Another device was evolved for the proposed development of distance drives. It permits the direct measurement of the total stress in the most endangered intermediate shafts. This device has already been successfully used in several cases. (Figs. 6 and 7.)

The reciprocal torsion of the two tested cross sections, I-I and II-II is measured with a torsion-proof indicator tube fitted on the shaft, following current torsion-indicator practice. The reciprocal torsions of the two cross sections being very small over comparatively short lengths of measurement (9.4 to 15 in.), the glass-scratch-recording method (reference 3) specially suitable for very short lengths, was used in this case. The records, like those of the torsigraph, are plotted full-scale and are not affected by inertia. The recording plate is driven by an electric motor (3), revolving with the shaft and supplied with current through a slip ring (10). In its present form, the whole measuring unit, made of two parts, can be fitted by interchangeable tightening rings on shafts of up to 80 mm diameter. The length of measurement can also be adapted to the various degrees of torsion by using indicator tubes of different lengths.

Greatly magnified records are shown in Figures 8a and 8b. In case a an almost as great alternating stress is superposed on the static load of the shaft portion due to the mean torque. Conditions are much more favorable in case b, measured on a distance-drive shaft. The superposed vibration stress is only a very small fraction of the mean torque which can very accurately be measured in this case.

The stress conditions in the smooth running and highly stressed intermediate shafts of distance drives will usually be as favorable. This affords another possibility of using the torsion recorder as an actual torque and power measuring device. Seen from this angle the comparatively simple and inertia-proof measuring installation may also be successfully used for shafts of ships and airships.

An improved type of the torsion recorder now in operation is shown in Figure 9. This device again incorporates the film-scratch-recording method successfully used in the first D.V.L. torsigraph, after it had been shown experimentally that sufficiently thin lines (to within 0.01 mm) can be plotted by this method. Considering the available length of measurement, the torsion of distance drive shafts is not likely to drop below this limit.

The device closely follows the general lines of the D.V.L. torsigraph. The film is again driven by the revolving shaft through a worm gear. The worm is stopped by a band brake with Bowden cable. This unit is extremely

handy and greatly reduces the revolving masses as compared to the experimental type. (Figs. 6 and 7.)

III. EXAMPLE: VIBRATION TEST OF A SIMPLE DISTANCE DRIVE

The test was made with the simple distance drive shown in Figure 10, consisting of a BMW IV engine - rubber coupling - lengthening shaft ($l = 150$ cm) - propeller. Although the test arrangement was simple, the results show that a stress calculation, based on the calculated form of vibration and on torsion graph measurements at the free shaft end only, is very contradictory as regards the stresses in the lengthening shaft. Not before the torsion recorder was used for the measurements could reliable figures regarding the true stress conditions be obtained.

The rubber coupling, the characteristics of which were determined by a torsion test (fig. 11), had a decisive influence on the vibration conditions of the installation. The diagram shows the departure from the linear law and the damping capacity of the coupling. About 15 per cent of the absorbed energy of deformation is retained during the discharge and converted into heat. The damping was determined by graphic differentiation of the work of deformation-load curve (radius = $f(M_d)$) as a function of the load (c and $l = f(M_d)$) and likewise plotted in Figure 11.

Figure 12 shows the equivalent vibration arrangement of the distance drive for a smooth shaft with an inertia moment $J_{p_0} = 242$ cm⁴. The assumed elastic length of the rubber coupling thereby corresponds to the load applied by the mean torque of the BMW IV engine (approximately 125 m kg). The damping of the coupling is comparatively soft. It equals that of a steel shaft of ~ 4.7 m length and ~ 70 mm diameter.

The single and double node vibration of the installation was calculated and plotted in Figure 12 with the respective natural vibration numbers $n_{e_1} = 2000$ 1/min. and $n_{e_2} = 6080$ 1/min. The only critical vibration likely to occur in the operating speed range of the installation, for the form of vibration n_{e_1} , is $n_{e_1}/3$, assuming roughly identical amplitudes of vibration in each crank. In spite of the proximity of the 1.5 harmonic at full throttle, any resonance with it is not likely to be very

pronounced. The form of vibration n_{e_2} , with a node closely before the rubber coupling, corresponds to the usual form of vibration of the engine with direct-drive propeller. (Fig. 1.) Hence, the well-known series of critical conditions $n_{e_2}/4.5$; $n_{e_2}/6$, ... appears in the operating speed range.

Following the preliminary vibration calculation, the installation was tested simultaneously at the free end of the engine crankshaft with a D.V.L. torsigraph and in the lengthening shaft with the torsion recorder. (Fig. 10.) Two records each, plotted with the two devices at the same time and speed, are shown in Figure 13.

The estimation of the test results in Figure 14 requires no further comments. It will be noted that, as anticipated, the critical condition $n_{e_1}/1.5$ is very little pronounced, whereas the critical $n_{e_1}/3$ is strongly marked in spite of greatly reduced engine speed. It is, furthermore, noteworthy that the natural vibration numbers n_{e_1} and n_{e_2} , calculated from the ordinal number and position of the critical vibration, differ materially from each other. This phenomenon is attributable to the anharmonic character of the rubber coupling, the elasticity of which changes with the mean torque exerted on it. (Fig. 11.) The engine was throttled down during the vibration measurement, the stiffness of the coupling thus increasing with the torque.

The following conclusions were reached by comparing the stresses in the lengthening shaft ($m\text{ kg}_1$ and $m\text{ kg}_2$), measured by the torsion recorder, with the stresses calculated on the basis of torsigraph measurements (φ_1 and φ_2) for the free vibrations n_{e_1} and n_{e_2} (fig. 12):

- a) In the strongly pronounced critical condition $n_{e_1}/3$, a calculated stress of $\pm 193\text{ m kg}$ corresponds to a measured stress of $\pm 176\text{ m kg}$. The true stress is less than 10 per cent below the calculated value. The small difference is attributable to the damping of the coupling but, under some conditions, may also be due to inaccuracy of measurement.
- b) A stress of $\pm 83\text{ m kg}$ is calculated from the slightly pronounced critical condition $n_{e_1}/1.5$, the measured value being $\pm 147\text{ m kg}$. In this case the

true stress is approximately 75 per cent above its calculated value and it is clear that for little pronounced critical conditions the stress calculation can no longer be based on the free form of vibration. In the present case the forced vibration is far from agreeing with the free vibration.

- c) In the critical condition $n_{e_2}/6$ the measured stress of ± 44 m kg is only ~ 20 per cent of the calculated stress of ± 200 m kg.
- d) In the critical condition $n_{e_2}/4.5$ the measured stress of ± 62 m kg is only ~ 40 per cent of the calculated stress of ± 160 m kg.

For resonances with n_{e_2} the true stresses of the lengthening shaft are obviously much smaller than those to be anticipated from stress calculations based on the free form of vibration n_{e_2} . If the internal damping of the rubber were proportionate to the frequency, this phenomenon might be attributed to a considerably increased damping effect of the coupling for the greater vibration number n_{e_2} . This assumption, however, is not admissible, since the material damping for a given amplitude of vibration is independent of the frequency. In this case it is probably a partial vibration of the engine gear proper reaching up to the node just before the rubber coupling. This vibration scarcely passes through the coupling, so that no material stresses of the form of vibration n_{e_2} are set up in the lengthening shaft. The example shows clearly that a completely wrong picture of the true stress conditions in the lengthening shaft would have been obtained without the measurement with the torsion-recording device.

IV. RESULTS OF VIBRATION TESTS WITH AIRCRAFT ENGINES

During the last few years the D.V.L. has investigated the vibration conditions of a large number of straight-type, V-type and radial aircraft engines. The free form of vibration and the relative vibration diagram of these engines were calculated. The true vibration diagram was plotted with a D.V.L. torsigraph at the free end of the crankshaft and the additional vibration stress was calculated as far as possible with the aid of the free form of vibration.

Various engines, with and without reduction gear and vibration-damping devices, with rigid and spring couplings connecting crankshaft and propeller, were tested in this manner. The vibration test revealed the effect of these different arrangements on the vibration characteristics. Further details regarding the position of the natural vibration numbers, the distribution of the critical points in the operating speed range and particularly the magnitude of the additional vibration stress of these engines were thus obtained.

Some of the test results are shown in Table I. In addition to the characteristics of the various engines, the principal torsional vibration characteristics are given in columns 5 to 12.

1. Natural Vibration Numbers

Column 5 gives an idea of the natural vibration numbers. The following distribution is obtained for direct-drive engines, using different values not contained in the table:

4-cylinder in-line engines	$n_{e_1} = 10900$ to 13900 1/min
6-cylinder in-line "	$n_{e_1} = 5900$ " 6600 "
12-cylinder V-type "	$n_{e_1} = 5400$ " 5740 "
Radial "	$n_{e_1} = 8800$ " 29000 "

In older engines of the same construction and similar power range these figures are unaffected by vibration considerations and do not vary much. The influence of vibration on the size of the crankshaft and gear components has been revealed of late by new engine types.

The natural vibration numbers are greatly cut down by reduction gears, usually much more than may be expected on the ground of the additional damping action of the gear shaft which must be reduced by the square of the gear ratio. As already mentioned in paragraph I,1, this phenomenon is attributable to the incorporation of the gear bearing and housing in the vibrating system. A preliminary calculation of the natural vibration number of geared engines, based on design drawings, is therefore hardly reliable.

In working out the dimensions of the damping mass which revolves with the system, the reduction, shown in column 5, of the natural vibration number by an additional vibration-damping device, must be taken into account. Owing to the often rapid succession of critical conditions, a too-heavy damping mass may introduce damped critical vibrations, originally lying outside the operating speed range, within this range.

The ordinal numbers of the most strongly pronounced critical conditions in the operating speed range are given in column 6. The table shows that resonance occurs at comparatively low harmonics with correspondingly large exciting amplitudes. An improvement may be achieved by increasing the natural vibration numbers to a level where resonance occurs only at major harmonics with respectively smaller excitation. Good results may be obtained only provided the crankshafts are much larger than those now currently used. The new method developed for straight-type engines may often be a satisfactory solution. It implies a comparatively low natural vibration number, additional damping and no material increase of weight (Section IV, 3, d). The natural vibration number of radial engines, the lowest critical condition of which corresponds to one-half its number of cylinders, may in certain cases be greatly reduced by additional intermediate damping members, as shown by Figure 15. In one case, the natural vibration number of a 9-cylinder radial engine was so far reduced ($n_{e_1} = 3400$ l/min) by a spring coupling between the crankshaft and the propeller and by elastically hinged counterweights that, although the lowest critical condition $n_{e_1}/4.5$ still occurred, it lay outside the regular operating speed range which is free from resonance. The vibration conditions of the 5-cylinder radial engine, which has a rather high natural vibration number ($n_{e_1} = 10600$ l/min), are far from being so favorable.

2. Vibration Stresses

The greatest vibration amplitude measured with the torsigraph, at the free end of the crankshaft, is given in column 7 of the table. This value, together with the free form of vibration, is the starting point for the stress calculation, the results of which are given in column 8. In all these cases but one, the additional vibration stress is a multiple of the static stress exerted on the shaft by the mean torque. (Column 9.) These figures show the decisive influence of the vibration conditions.

on the dimensions of the crankshaft. The stresses given in imkg do not yet permit of comparing the different engines.

Columns 10 and 11 show the magnitude and location of the additional vibration stress of the crankshaft, referred to the cross section with the smallest antitwisting moment, irrespective of stress increments due to special forms of the shaft, stress cumulation at changes of cross section, notch effect, inherent stresses, etc. A reliable calculation of these influences is hardly possible. They must be directly determined by stress measurements with extensometers having a very short stroke and facilitating access to points of great stress accumulation (hollow throats, notches, etc.). In the absence of such investigations it must be assumed at first that all the tested crankshafts are equally subject to the above influences. Then, the figures of column 10 permit of a first comparative estimation of the various engines. Inasmuch as the true resistance of the crankshaft to alternating stresses is not known and the alternating strength characteristics of smooth test pieces (approximately 37 kg/mm^2) or model crankshafts (approximately 20 kg/mm^2) are not convertible to full-scale parts, it was hitherto impossible to estimate the absolute admissible ultimate stress withstood by the shaft without failure. Sustained torsion tests of the actual crankshaft, for the determination of its true resistance to alternating stresses, are therefore urgently recommended. Such tests would also agree with the new tendency of applying dynamic stress investigation methods to full-scale tests with completed parts. An installation for the testing of crankshafts in their respective bearings and housings at their operating vibration number and form (fig. 1) is now under development at the D.V.L.

Until the first test results become available, at least an approximately correct scale of comparison, of practical use, is urgently needed. The danger of failure may be estimated, with certain restrictions, on the basis of the statistics of failures in column 12. The assumption is justified that the composite stress causing the failure of the shaft consists chiefly of the torsional vibration stress which exceeds all the other components (bending, inherent stresses, etc.). Then, by comparing columns 10 and 12, a stress of approximately 6 kg/mm^2 may be derived which, at present, stands for the statically determined admissible limiting stress. Owing to the above

assumptions this figure must be used with discrimination as a basis for estimates. This substitute will have to be used until further details become available. On the other hand, the persistent lack of reliability in estimating the danger of failure, increases the urgency of full-scale tests with actual crankshafts.

3. Vibration Damping

In connection with the vibration stresses of aircraft engines, vibration damping, at present the best-known means of reducing these stresses, is briefly referred to below. A greatly simplified diagram of the various types of vibration-damping arrangements is shown in Figure 16. The various masses and springs of the power plant shown in the figure are concentrated in one mass m_1 and one spring unit c_1 connected with the very large propeller mass M .

a) Resonance pendulum.-- The designation "vibration damper," by which this device is sometimes designated, is incorrect, since the vibration energy is not damped or destroyed ($D = 0$). Hence, the resonance pendulum is shown only as a transition to the damping device b . Device a is a small coupled pendulum $c_2 m_2$, in resonance with the system $c_1 m_1$ which is to be damped. According to the theory of the double pendulum in this case,

$$x_1 = 0$$

$$x_2 = -\frac{E}{c_2} \sin \omega t$$

at the original point of resonance $\omega = \sqrt{c_1/m_1}$ of the system $c_1 m_1$. Resonance is thus eliminated at this point but replaced by two new resonances, one below and the other above it. The original point of resonance ω is approached the closer by these new resonances, the smaller c_2 and m_2 are as compared with c_1 and m_1 . Hence, the resonance pendulum is only a remedy for engines with constant revolution speeds at a certain critical condition. As a rule, the running conditions of aircraft engines, which have a rather wide operating speed range, are not improved by a shifting of the critical vibration point, but only by its elimination by transformation of the vibration energy into heat.

b) Resonance damper.- This device produces the required damping action D , which should have the optimum value (D_{opt}) between $D = 0$ and $D = \infty$. A damper of this type, designed for aircraft engines, was recently proposed by O. Föppl (reference 4) and is now under development. Instead of an external damping force, Föppl uses the internal damping of the spring c_2 , which is best made of rubber.

c) Friction damper.- In this case $c_2 = 0$ and the damping mass m_2 is coupled with m_1 by solid or viscous friction only. Even in the optimum position (D_{opt}) the action of this damper, for the same weight, is less than that of the resonance damper b which increases the relative path $x_2 - x_1$ by the resonance of the damping pendulum $c_2 m_2$.

Device c was hitherto used as a friction or liquid damper only for aircraft engines. As shown by several examples in Table I, these dampers have, by long experience, been developed into the most efficient means of reducing undue vibration stresses. Crankshaft failures are prevented on engines (especially 6-cylinder straight-type) equipped with dampers.

As a rule the damping devices b and c are mounted on power plants developing vibrations in operation. As individual units, mounted on a free end of the shaft (external dampers), their use, which increases the weight of the engine and remains an emergency solution, is justified only when other means for eliminating the danger of vibration are not available.

d) Internal damping*.- Unlike external dampers, the damping unit roughly described in this paragraph, is incorporated from the beginning in the power plant. A strong damping action is achieved by using the great propeller mass M as the damping mass m_2 , without thereby increasing the weight of the engine. It is still rather difficult to form an opinion on the new solution introduced by internal damping. Yet, according to the vibration diagram of Figure 17, which is nearly free from resonance, and was plotted for an aircraft engine with internal damping, this solution of the vibration problem seems to be good, especially for an optimum adjustment of the damping unit (D_{opt}).

*The designation "internal damping" was taken over from Professor Junkers' Research Institute which, first in Germany, applied this kind of damping to airplane engines.

V. SUMMARY

A knowledge of the vibration and stress conditions in flight is essential for judging the reliability of aircraft engines, based on the free form of vibration and on the relative and true vibration diagrams. As a rule, the free form of vibration and the relative vibration diagram may be calculated in advance with sufficient accuracy. The vibration conditions of running engines may thus be predicted and the necessary improvements introduced in time.

True vibration diagrams are usually obtained from vibration measurements on the completed engine. Two devices for this purpose and supplementing each other, the D.V.L. torsigraph and the D.V.L. torsion recorder, are described in this report. The D.V.L. torsigraph, mounted at the free end of a shaft, measures the vibrations of the latter with respect to a uniformly revolving mass, while the torsion recorder measures directly the reciprocal torsion of two shaft cross sections and hence the total stress (mean torque and superposed vibration stress). An investigation of the vibrations of a simple distance drive by means of the two devices is given as an example.

Several final results and the discussions of vibration tests are added. Attention is called particularly to the still-prevailing uncertainty regarding the estimation of admissible vibration stresses and to the consequent necessity of determining the true alternating strength of crankshafts by full-scale tests. Until such results become available, a statically determined limiting stress is suggested as a temporary criterion. Vibration damping, the best means of reducing the vibration stress known at the present time, is briefly referred to in this connection.

Translation by W. L. Kaporindé
National Advisory Committee
for Aeronautics.

REFERENCES

1. Brandt, R.: "Untersuchung über die Erregung von Dreh-
schwingungen in Reihenmotoren. D.V.L. Report No.
210. Jahrbuch 1931, D.V.L., pp. 343-357.
2. Stieglitz, A.: "Der D.V.L. Torsiograph; ein Drehschwing-
ungsmessgerät für Fahrzeugmotoren." D.V.L. Report
No. 204. Z.F.M., Vol. 22, No. 2, 1931, pp. 49-52;
and Jahrbuch 1931, D.V.L., pp. 358-361.
3. Pabst, W.: "Aufzeichnen schneller Schwingungen nach dem
Ritzverfahren." D.V.L. Report No. 167. Z.V.d.I.,
Vol. 73, 1929, p. 1629; and Jahrbuch 1930, D.V.L.,
pp. 31-36.
4. Föppl, O.: "Resonanzschwingungsdämpfer." Ingenieur-
Archiv, Vol. II, No. 3, 1931, pp. 347-352.

TABLE I. TORSIONAL VIBRATION CHARACTERISTICS OF VARIOUS AIRCRAFT ENGINES

Engine Characteristics			Torsional Vibration Characteristics							Remarks	
1	2	3	4	5	6	7	8	9	10	11	12
Number and setting of cylinders	Power hp	Mean crankshaft torque M_{cs} mkg	Remarks	Fundamental vibration number n_1 /min	Orderly number of highest critical condition in speed range	Max. vibration amplitude in crankshaft end $\pm \varphi$	Max. vibration stress in crankshaft \pm mkg M_{cs}	$\frac{M_{cs}}{M_{cm}}$	Max. theoretical vibration stress T_s of crankshaft \pm kg/mm ²	Point of T_s	Remarks
4-cyl. in-line	100	35		10900	6	1.6	146	4.2	5.8	1st throw	No failure known; critical condition to be avoided
6-cyl. in-line	235	119	Without vibration damper	5900 (2300)	4.5 (1.5)	2.6	473	4.0	14.2	Propeller pin	Repeated failures. No further failure.
	280	141	With vibration damper.	6200 (5550)	4.5 (4.5)	2.25	464	3.3	13.8	1st throw	Repeated failures. No further failure
8-cyl. V type	325	145	Without vibration damper	6600 (4260)	4.5 (3)	3.0	768	5.3	13.8	1st throw	Repeated failures. No further failure.
	400	128	Reduction gear	4350	3	1.3	290	2.0	5.2	1st throw	Engine not in regular use, danger of failure.
12-cyl V type	200	74		9550	5.5 (4)	0.6 (2.2)	152	2.1 (7.5)	4.5 (16.4)	1st throw	Engine not in regular use. Critical condition of fourth order (figures in brackets) lies outside cruising-speed range.
	500	249	Direct drive	5400	3.5	1.75	489	2.0	7.1	1st throw	Occasional failures.
12-cyl V type	500	239	Reduction gear	4700	3	1.83	405	1.7	5.9	1st throw	One failure known, can not be used for criterion; cause of failure being uncertain.
	600	270	Direct drive	5740	6	1.15	436	1.6	5.6	Propeller pin	
5-cyl. radial	620	283	Without vibration damper	4500	3	1.6	416	1.5	4.1	Between reduction gear & first throw	Engines only short time in use; judgment not yet possible. No failure known.
	76	30	With reduction gear	2200	(1.5)	0.9	210	0.7	2.0		
9-cyl. radial	200	80	Elastically attached propeller and shock-absorbing counterweight	3400	4.5	0.72	172	2.2	-	Propeller pin	Critical condition not reached; no failure reported.
9-cyl. radial	480	194	Reduction gear	3710	4.5	1.54	299	1.5	6.1	Throw	No failure reported. Engines only short time in use; judgment not yet possible; critical condition to be avoided.

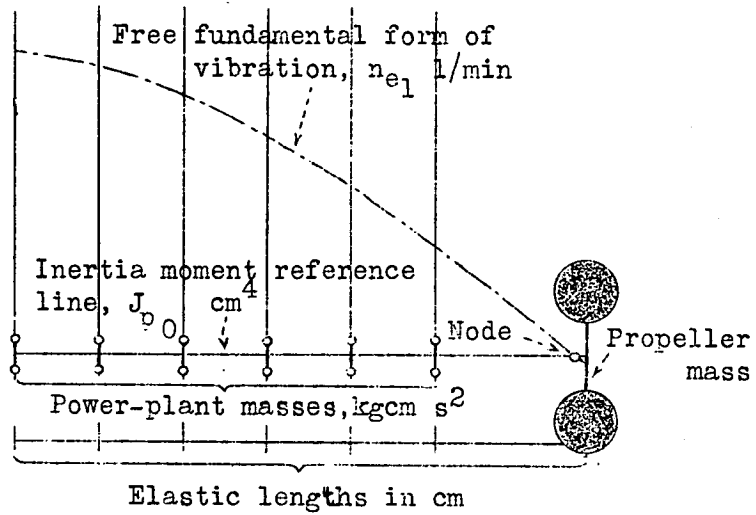


Fig. 1 Vibration arrangement and free fundamental form of vibration of a six-throw aircraft engine with propeller.

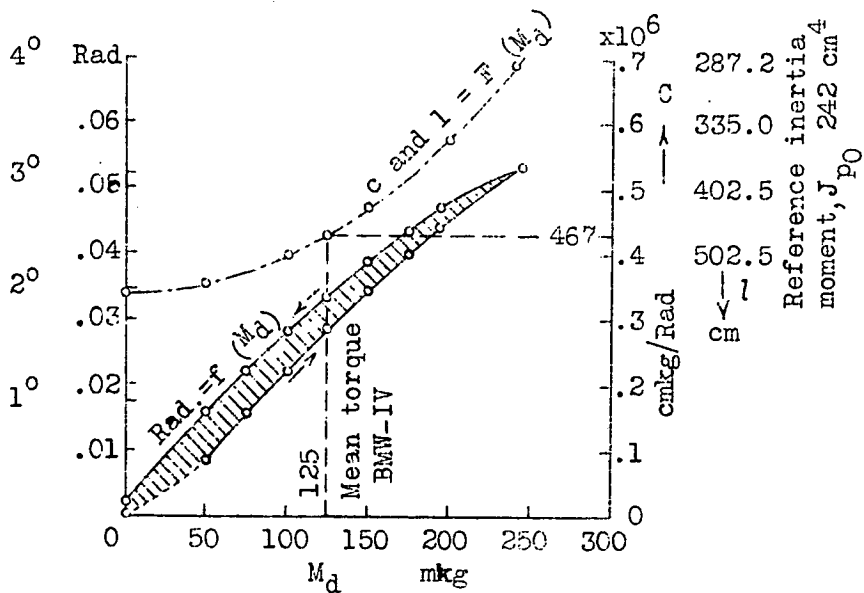


Fig. 11 Spring action and damping of rubber coupling.



Fig. 2 Torsio-
graph
with film scratch
recording device.
Large and small
type.

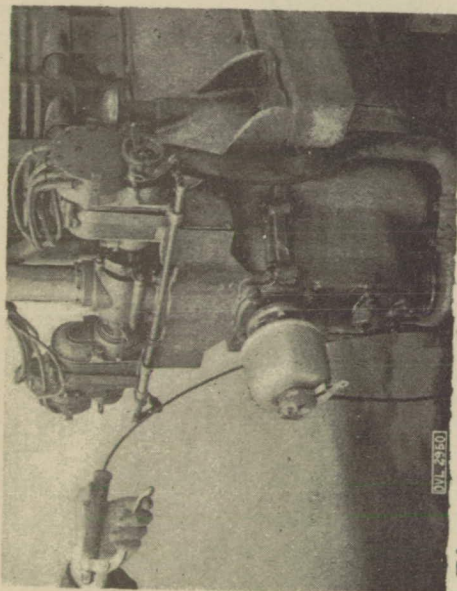
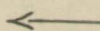


Fig. 4 Small DVL torsionograph,
with distance brake,
flanged to the crankshaft of an
aircraft engine.

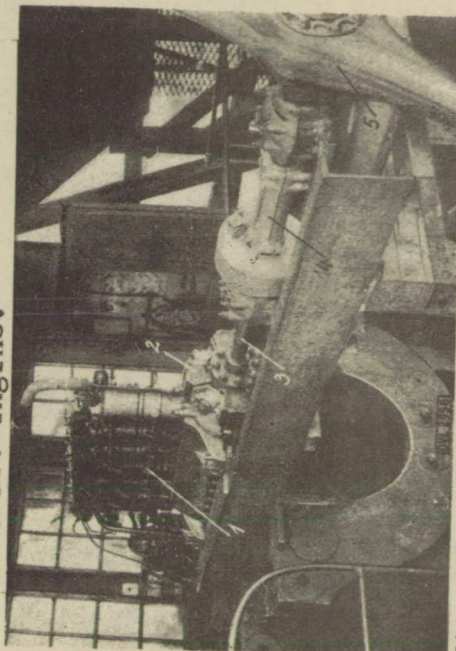


Fig. 10 Experimental distance drive.
1. B.M.W.-IV engine. 2. Rub-
ber coupling. 3. Lengthening shaft (L
= 150 cm). 4. Built-in torsion record-
er. 5. Propeller.

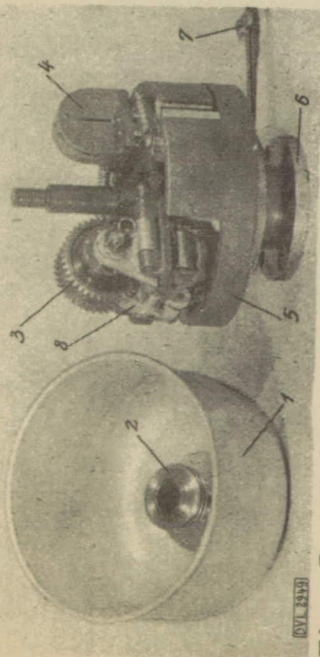


Fig. 3 Small DVL torsionograph with
housing removed. 1. Housing.
2. Film worm drive. 3. Worm gear.
4. Film holder. 5. Uniformly revol-
-ing torsionograph mass. 6. Attach-
-ment flange. 7. Wires supplying cur-
-rent for time and revolution marks.
8. Film.

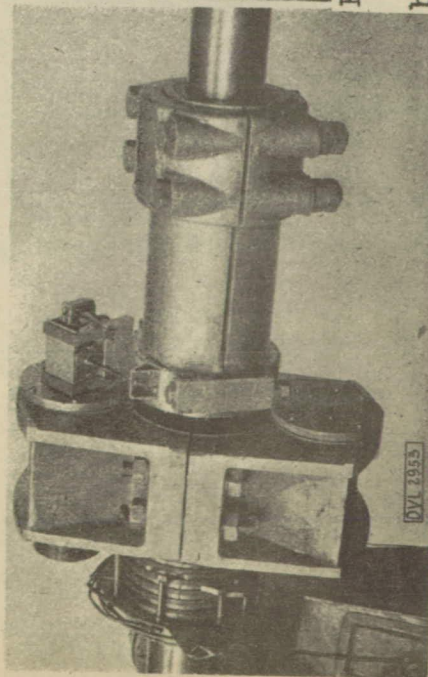


Fig. 7 DVL glass scratch torsion
recorder.

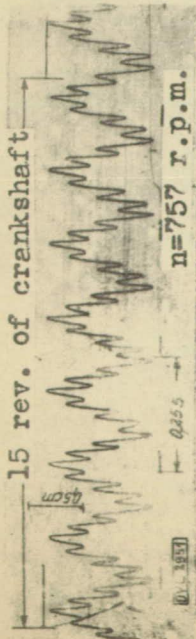
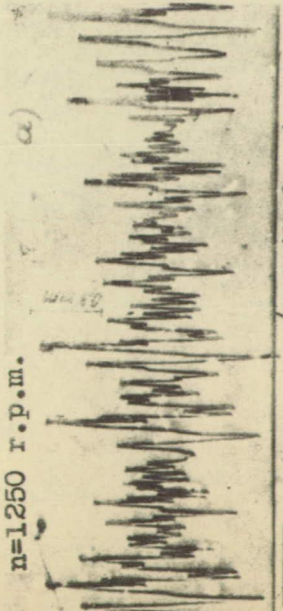


Fig. 5 DVL torsigraph record with time and revolution marks. (slightly enlarged)



n=1250 r.p.m.

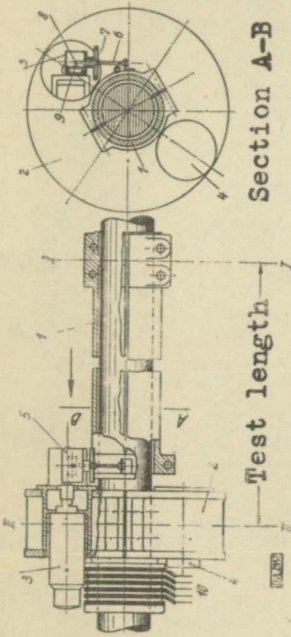


Fig. 6 DVL glass-scratch torsion recorder.
1. Indicator tube mounted in test cross section I-I.
2. Counterpart mounted in test cross section

Section A-B

Test length

II-II. 3. Electric motor driving glass plate and revolving with shaft. 4. Counterweight. 5. Recording head. 6. Push rod for recording diamond.

Fig. 8 Records plotted with DVL glass scratch torsion recorder (much enlarged). a) recorded on test stand. b) recorded with distance control on airplains. $M_{dm} =$ mean torque. M_{ds} = superposed vibration stress approx. $1/20 M_{dm}$ M_{da} = starting stress approx. $+ 3 1/2 M_{dm}$. M_{dr} = kicking stress approx. $- 1.3 M_{dm}$.

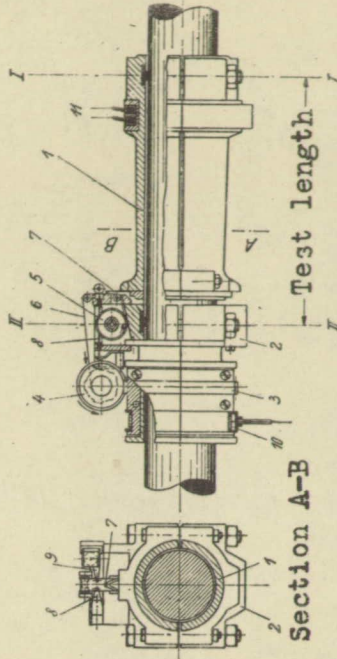
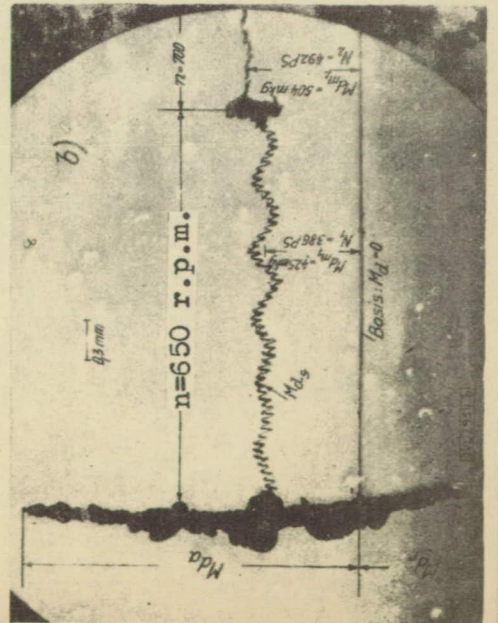
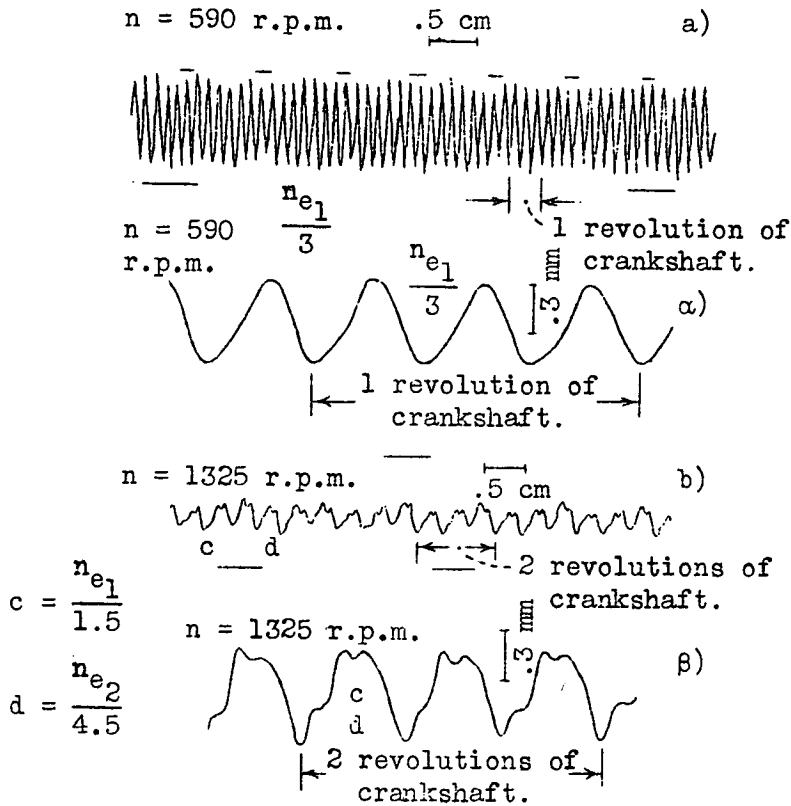


Fig. 9. DVL film scratch torsion recorder. 1. Indicator tube mounted in test cross-section I-I. 2. Counterpart mounted in test cross-section II-II. 3. Worm driving the film strip. 4. Worm wheel. 5. Film reel. 6. Film strip. 7. Recording diamond. 8. Mechanically driven revolution recorder. 9. Electrically driven time recorder. 10. Band brake with Bowden cable for locking the worm. 11. Current supply for the time marker.



n=650 r.p.m.

Basis: $M_d = 0$



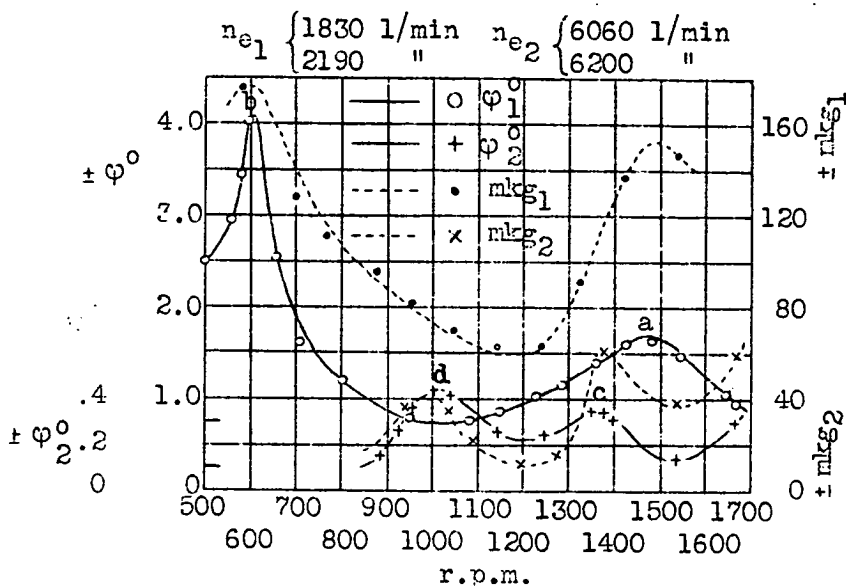
a) and b). Torsiograms at free end of crankshaft (slightly enlarged).

α) and β). Torsion diagrams of lengthening shaft (greatly enlarged).

a) and α). $n = 590 \text{ r.p.m.}$ critical condition $\frac{n_{e1}}{3}$

b) and β). $n = 1325 \text{ r.p.m.}$ critical condition $\frac{n_{e1}}{1.5}$ and $\frac{n_{e2}}{4.5}$

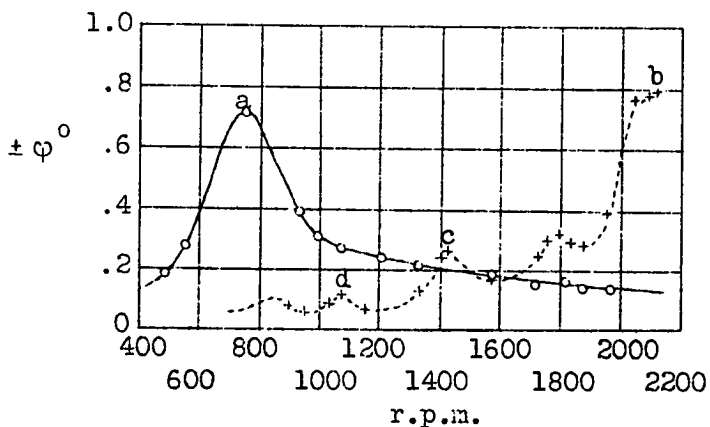
Fig. 13 Simultaneous records of the DVL torsigraph and of the torsion recorder.



$$a = \frac{n_{e1}}{1.5} \quad b = \frac{n_{e1}}{3} \quad c = \frac{n_{e2}}{4.5} \quad d = \frac{n_{e2}}{6}$$

Φ_1 and Φ_2 = vibration amplitudes at free end of crankshaft, corresponding to vibrations n_{e2} and n_{e1} . mkg_1 and mkg_2 = stresses in lengthening shaft, corresponding to vibrations n_{e1} and n_{e2} .

Fig. 14 Vibration and stress relations of experimental distance drive.

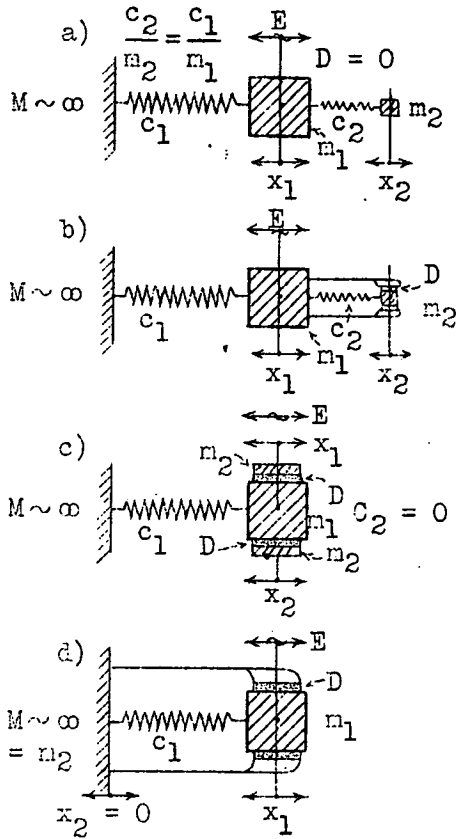


$$a = \frac{n_{e1}}{4.5} \quad b = \frac{n_{e1}}{5} \quad c = \frac{n_{e1}}{7.5} \quad d = \frac{n_{e1}}{10}$$

— 9 cylinder radial engine with damping propeller coupling and damping counter weights, $n_{e1} = 3400$ l/min.

----- 5 cylinder radial engine with rigid propeller coupling, $n_{e1} = 10600$ l/min.

Fig. 15 Vibration diagrams of two radial engines with large and small natural vibration numbers.



- a) Resonance pendulum.
- b) Resonance damper.
- c) Friction damper.
- d) Internal damping.

$M \sim \infty$ propeller mass.
 m_1 , joint power plant mass.
 c_1 , joint crankshaft damping.
 m_2 , damping mass.
 c_2 , damper spring.
 x_1 or x_2 vibration amplitudes of m_1 or m_2 .
 $E = E_{max} \cdot \sin \omega t$ vibration excitation (total turning force)
 D , damping force
 = const. (friction damping)
 = $\kappa (x_2 - x_1)$ (liquid damping)
 = $\frac{\kappa}{\omega} (x_2 - x_1)$ (material damping)

Fig. 16 Diagrams of vibration dampers.

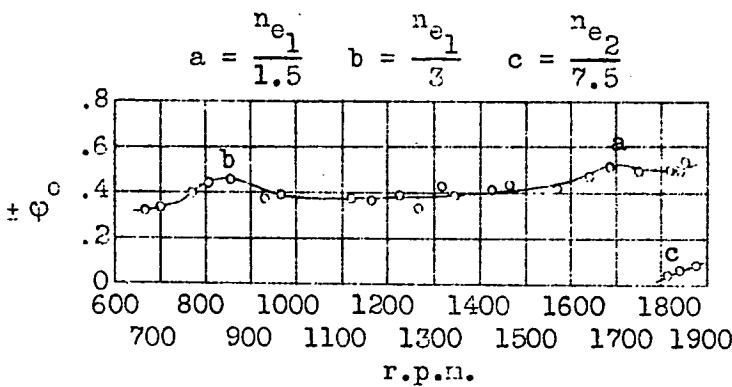


Fig. 17 . Vibration diagram of an aircraft engine with internal damping (Junkers L 88 engine). $n_{e1} = 2550$ l/min.